Nanoliter liquid characterization by open whispering-gallery mode dielectric resonators at millimeter wave frequencies

E. N. Shaforost, N. Klein, S. A. Vitusevich, A. Offenhäusser, and A. A. Barannik

Citation: Journal of Applied Physics **104**, 074111 (2008);
View online: https://doi.org/10.1063/1.2991182
View Table of Contents: http://aip.scitation.org/toc/jap/104/7
Published by the American Institute of Physics

Nanoliter liquid characterization by open whispering-gallery mode dielectric resonators at millimeter wave frequencies

E. N. Shaforost,[1,a)] N. Klein,[1] S. A. Vitusevich,[1] A. Offenhäusser, and A. A. Barannik[2]
[1]*Institut für Bio- und Nanosysteme and CNI–Center of Nanoelectronic Systems for Information Technology, Forschungszentrum Jülich, Jülich D-52425, Germany*
[2]*A. Usikov Institute of Radiophysics and Electronics, NASU, 12, Acad. Proskura str., 61085 Kharkiv, Ukraine*

(Received 24 June 2008; accepted 13 August 2008; published online 8 October 2008)

We present an approach for identification and concentration determination of liquids of pico to nanoliter volumes at a frequency of 35 GHz based on a whispering-gallery mode (WGM) dielectric resonator technique. A quasioptical coupling scheme based on dielectric image waveguides was employed to excite high-Q running wave WGMs with uniform azimuthal field distribution in cylindrical sapphire disks with quality factors up to 4×10^5 at room temperature. Measurement of the liquid induced changes in the resonator quality factor and resonance frequency has been performed for droplets down to 90 pl volume spotted at different positions on the surface of the sapphire disk. We have employed our method for concentration determination of ethanol, glucose, and albumin dissolved in water. Solutions with concentration values well below 10% could be clearly separated from pure water. Our method is promising for the characterization of biological liquids. © *2008 American Institute of Physics*. [DOI: 10.1063/1.2991182]

I. INTRODUCTION

The complex permittivity of liquids $\varepsilon^*(\omega)=\varepsilon'-i\varepsilon''$ at microwave and millimeter wave frequencies, in particular its frequency dependence measured over a broad range, is very specific to the chemical composition. Therefore, precise determination of $\varepsilon^*(\omega)$ can be employed for liquid identification in case of single component liquids and concentration determination in case of multicomponent liquids.

Broadband determination of the complex permittivity was performed by various microwave transmission line techniques both in reflection and transmission geometry.[1–3] In particular, reflection measurements by coaxial probes provide a simple and versatile technique for broadband characterization of liquids at microwave frequencies. Here the required volume is of the order of a few milliliters. Various approaches have been reported recently to reduce the volume of the liquid required for broadband measurement. Murata *et al.*[4] employed a variable capacitive gap between the inner conductors of two oppositely faced coaxial lines and demonstrated broadband permittivity measurements on thin films of 50–300 μm thicknesses. Furthermore, the integrations of microfluidic structures with coplanar waveguide transmission lines were reported recently,[5,6] which enable to measure the dielectric properties of submicroliter volumes of fluids and biological samples at frequencies up to 40 GHz. On the other hand, resonator measurements[7,8] provide a sensitivity that is approximately Q times higher than for nonresonant structures, with Q being the quality factor of the resonator.

Within our study we have explored the use of cylindrical dielectric resonators excited in so-called whispering-gallery modes (WGMs) with emphasis on future high frequency sensor applications up to terahertz frequencies. This type of resonators allows for the highest quality factors and thus for extraordinary high sensitivity for the determination of frequency shift and Q changes imposed by the object to be studied. In order to achieve the ultimate sensitivity the liquid should be positioned within the area of maximum electric field, as demonstrated by our results.[9]

WGMs are high-order azimuthal modes occurring when electromagnetic waves propagate inside a high permittivity and low-loss medium of circular geometry. The wave undergoes multiple total internal reflections at the resonator boundary along the perimeter and becomes confined inside the resonator, giving rise to resonances. The important features of total internal reflection are the presence of an evanescent wave outside the resonator very close to the boundary surface and almost negligible radiation losses in high-order WGM resonators.[10] Typically, for azimuthal mode numbers above six quality factors in the 10^4–10^5 range can be achieved in open unshielded resonator structures, if low-loss single crystalline or ceramic dielectric materials are employed.[11] The concept of WGMs can be employed from the low gigahertz range up to optical frequencies and therefore provides a challenging approach for highly sensitive broadband investigation of liquids.[12]

The study of the interaction of the excited electromagnetic resonant field with biological liquids has a potential to reveal important information about mechanisms responsible for common diseases, such as a cancer, and to show up advanced methods for medical diagnostics. WGM microcavities were successfully applied as miniaturized biosensors in the optical range for the identification and monitoring of proteins, DNA, peptides, and toxin molecules.[13–15] In our case, we utilize the relaxation of the water molecule in the liquid phase, which provides a characteristic broad peak in the dielectric losses between 5 and 50 GHz. Any organic or inor-

[a)]Electronic mail: o.shaforost@fz-juelich.de. On leave from the Institute of Radiophysics and Electronics, NASU, 61085 Kharkiv, Ukraine.

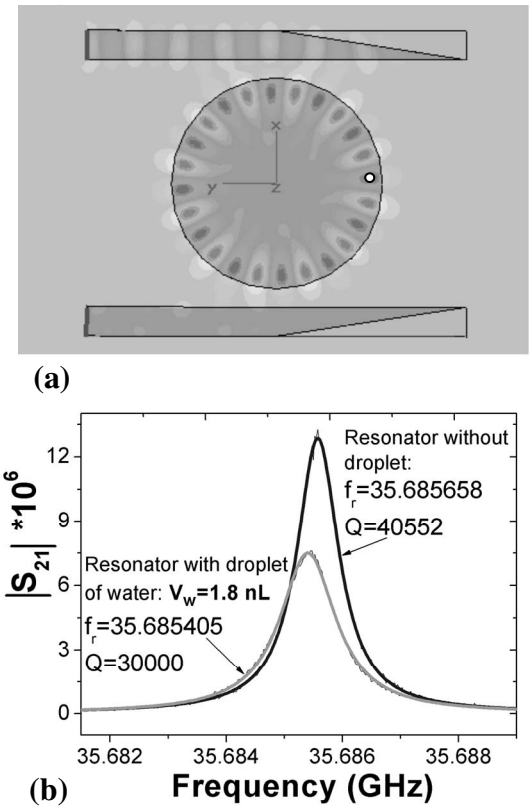

FIG. 1. (a) Simulated distribution of the electric field amplitude at resonance showing resonator disk and dielectric image waveguides. The optimum position of the droplet under test is indicated as a white circle. (b) Measured resonance curve before and after droplet spotting. The experimental data are fitted by Lorentzian curves.

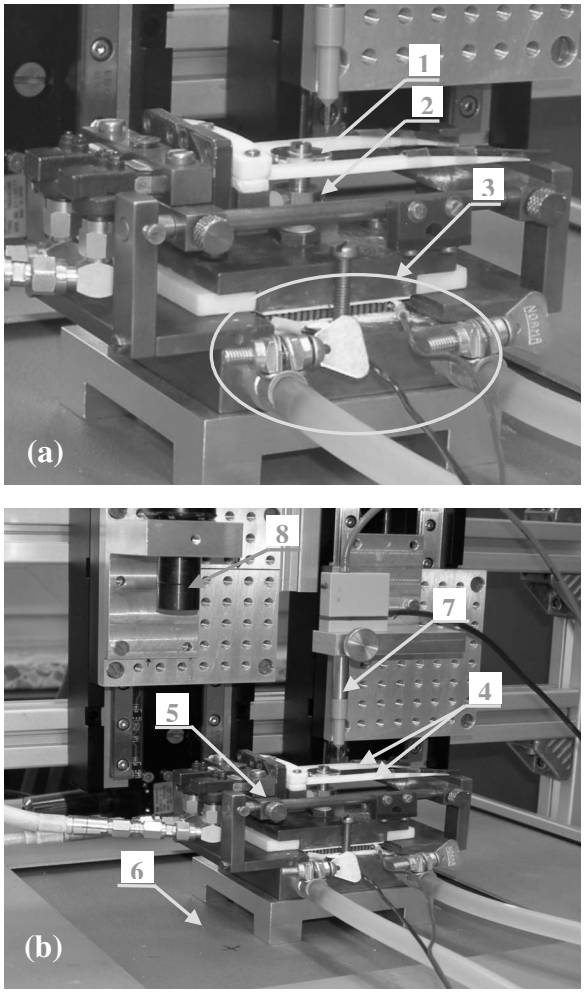

FIG. 2. (a) Photograph of the experimental setup in a close view. (b) A view of the resonator including spotting-positioning system. The main elements of the experimental setup indicated by arrows are: (1) resonator, (2) holder for resonator and temperature platinum sensor, (3) elements of temperature stabilizing system including a Peltier element and plate with circulating cooling liquid providing an effective extraction of heat, (4) dielectric waveguides, (5) mobile carriage utilized for positioning of the coupling elements, serving as their holder simultaneously, (6) *xy* scanning table, (7) *z* axis moving automated microinjection pipette, and (8) miniature charge coupled device camera.

ganic dissolved molecules in water will result in a decrease in the concentration of "free" water molecules contributing to the relaxation losses and change in the intermolecular bonds. Therefore, we expect that our method based on WGM will be suited for characterization of water-biosubstance solutions in very small volumes.

II. EXPERIMENTAL DETAILS

Within our approach, we have investigated various substances dissolved in water in the shape of a droplet of volume down to 90 pl, which was prepared by a microprocessor controlled microinjection pipette and spotted onto the most sensitive position on the WGM resonator surface according to the calculated field distribution in the resonator [see Fig. 1(a)]. The droplet leads to a significant reduction in quality factor and shift of resonance frequency as it is demonstrated by Fig. 1(b) for the case of a droplet of bidistilled water. The selected frequency of 35 GHz is slightly above the maximum of water absorption, and therefore provides suitable conditions for detection of small amounts of water with respect to a compromise of the short wavelength and the high water absorption. The signal transmitted S_{21} from the input to the output waveguide through the resonator depicted in Fig. 1 (absolute value of S_{21}) around the resonance frequency was measured with a Hewlett-Packard 8722C vector network analyzer. The HP 8722C was interfaced with a computer using HTBASIC 9.5 and a General Purpose Interface Bus (GPIB) controller to measure and store the data. Measurements were always performed approximately five times for the same droplet volume of each liquid under test.

The resonator assembly was composed of the sapphire resonator, resonator holder, coupling elements, and a Peltier cooler based system for temperature stabilizing as shown in the photograph (Fig. 2). The resonator assembly was attached to an *xy* scanning table through a metal holding plate as it is shown in Fig. 2(a). A computer controlled spotting-positioning system employs the scanning *xy* table for precise positioning of the resonator system in front of the nozzle tip of a fine glass capillary connected to an autodrop pipette system. AD-K-501 pipette is based on a piezodriven inkjet printing technology, and the smallest droplet, which is emitted from the nozzle tip and detected by our resonator system, has a volume of about 90 pl. The spotting system is also equipped with a miniature camera setting for controlling the droplet shape. For the purpose of stabilizing the droplet on

the resonator surface and avoiding rapid evaporation of the liquid from the surface as well as for stabilization of the dielectric resonator characteristics, a temperature controlling system was utilized to keep the temperature of the resonator at 18 ± 0.1 °C, which was slightly lower than the temperature of 23 °C in the laboratory.

Coupling of electromagnetic wave to the sapphire resonator disk was achieved by overlapping of the evanescent radiation field of the WGM with the evanescent field of dielectric image waveguides made of teflon and optimized for the best coupling of the resonator at the frequencies of interest [see Fig. 1(a)]. For input and output coupling, we employed dielectric image waveguides[16] (one side being metalized) of rectangular cross section, each of them was tapered at the end and introduced into a metal waveguide, which was connected to the network analyzer via a commercial waveguide-to-coaxial adaptor.

The measurements on the resonator of transmission type were performed under conditions of weak coupling such that measured resonant frequency and quality factor are not significantly affected by the coupling. The adjustment of coupling elements with respect to the resonator was carried out with a mobile carriage where these elements were fixed, such that the measured resonant curve of the resonator without droplet becomes closer to an ideal Lorentzian.

III. ELECTRODYNAMIC PROPERTIES OF OPEN WGM-DIELECTRIC RESONATOR WITH A SMALL WATER DROPLET

Our preliminary studies[17] were performed with WGM-type sapphire resonators shielded by a semiopen metal housing. In that case, coupling was performed by coaxial loops such that standing wave–type WGMs were excited in the sapphire disk. However, coaxial loops cannot be used for the case of millimeter-submillimeter bands, and integrated resonator arrays cannot be realized in this manner.

As mentioned in Sec. II, we employed distributed coupling by dielectric image waveguides, which makes it possible to excite running waves in an open resonator structure without any shielding and can work at frequencies up to the infrared range. Our results on droplets are presented as droplet induced change in the inverse quality factor (corresponding to losses induced by the droplet) and resonant frequency shift as illustrated in Fig. 3, which shows the experimental results for a droplet of about 2 nl volume at different positions on the surface of the resonator. The droplet position was varied along the azimuth (along the semicircle of the disk) at a fixed radial coordinate corresponding to the maximum strength of the electric field. The radial dependencies for both resonator characteristics at a fixed azimuthal position of maximum of electric field are inserted in Fig. 3.

The dependencies shown in Fig. 3 exhibit a very good agreement with the simulated field distribution of the $HE_{n1\delta}$ WGM (quasi-TM-type providing dominant electric field aligned along the cylinder axis) with azimuthal mode number $n=12$, which was excited in the resonator. For this mode the dependencies shown in the insert of Fig. 3 reflects the radial distribution of the square of the electric field $\boldsymbol{E}^2$. For an ideal running whispering-gallery wave one would expect

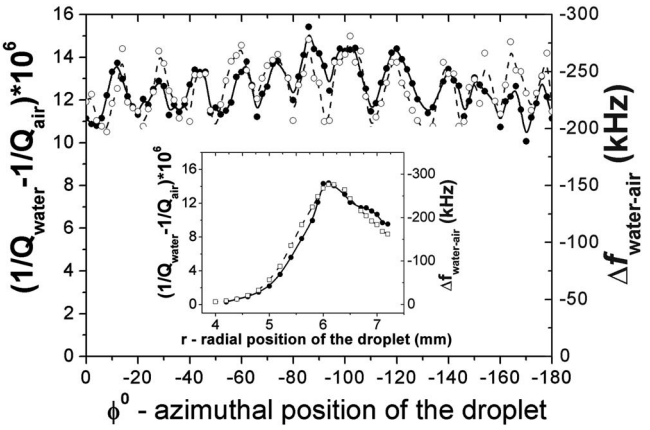

FIG. 3. Measured water droplet induced changes in inverse quality factor $1/Q_{\mathrm{wat}} - 1/Q_{\mathrm{air}}$ (solid circles) and resonant frequency $\Delta f_{\mathrm{wat\text{-}air}}$ (open squares) as functions of the droplet position varied in the azimuthal direction at a fixed radial position $r=6.1$ mm. Insert: the radial dependence for the same parameters at a fixed position of azimuth $\varphi=86°$. The volume of water droplet was 1.8 nl ($T=18$ °C).

no field variation in azimuthal direction, the observed 20% periodic variation in $\boldsymbol{E}^2$ indicates that 80% of the resonant energy is stored in a running wave mode. The maxima in these dependencies display the most sensitive areas for droplet positioning and correspond to the twelve antinode areas of the simulated field distribution illustrated in Fig. 1(a). Further optimization of the dielectric waveguides and matched loads can provide more uniform dependence of the field amplitude on azimuthal coordinate. The advantage of running wave excitation is that the droplet position becomes independent on the azimuthal coordinate, such that there is no need for precise positioning of the small liquid droplet in the azimuthal direction. This result is very important, particularly if we extend our approach to submillimeter frequencies where the resonator dimensions are smaller. The excitation of a running WGM wave by dielectric waveguides describes an attractive approach for integrated terahertz WGM resonator arrays for biosensing applications in the future.

In order to optimize the amount of liquid to be tested, we have measured the dependencies of frequency shift and loss variation on the volume of the water droplet. For that purpose, droplets of different volumes were spotted onto the resonator surface at a position of maximum electric field, according to our simulated [Fig. 1(a)] and experimental (Fig. 3) maps. The results shown in Fig. 4 indicate almost linear dependencies of both frequency shift and loss variation on the droplets volume for droplets smaller than 2 nl. For larger volumes, the observed sublinear behavior can be explained from the fact that the droplet extends over a large surface area such that the field inhomogeneity should be taken into account (see Figs. 1 and 3).

Droplet induced changes in the inverse quality factor $\Delta(1/Q_{\mathrm{liq\text{-}air}})$ were determined by two different ways. As the first method we used the equation,

$$\Delta\frac{1}{Q_{\mathrm{liq\text{-}air}}} = \frac{1}{Q_{\mathrm{liq}}} - \frac{1}{Q_{\mathrm{air}}},$$

where $Q=f_r/\Delta f_{1/2}$ was determined from the resonance frequency f_r and the halfwidth $\Delta f_{1/2}$. Although the so-called "3

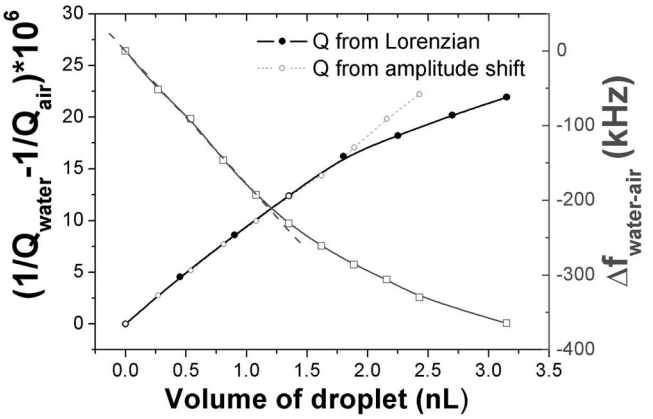

FIG. 4. Measured water droplet induced changes of resonant frequency $\Delta f_{\text{wat-air}}$ (squares) and inverse quality factor $1/Q_{\text{wat}}-1/Q_{\text{air}}$ (circles) as functions of droplet volume ($T=18$ °C).

dB" method is used often to determine Q, we obtained more accurate results by fitting the resonance curve to a Lorentzian.[18]

As an alternative method providing even higher accuracy for the smallest droplets we determined changes in the quality factor by measuring the decrease in the amplitude of the resonant curve at $f=f_r$,

$$\Delta\frac{1}{Q_{\text{liq-air}}}=\frac{1-10^{(\alpha_{\text{air}}-\alpha_{\text{liq}})/20}}{Q_{\text{air}}\times 10^{(\alpha_{\text{air}}-\alpha_{\text{liq}})/20}},$$

where $\alpha_{\text{air}}-\alpha_{\text{liq}}$ is the difference between the amplitudes in decibel.

IV. CHARACTERIZATION OF DILUTED AQUEOUS SOLUTIONS

Depending on the liquid composition we can describe several types of liquids with a specific behavior of the dielectric function. In one case, the strength of the electrical polarizability and the molecular relaxation, the latter being determined by the molecular mass and the intermolecular interaction, provides a fingerprint for semipolar liquids such as alcohols. In the other case, long chain hydrocarbons with a low real part of permittivity can be differentiated to some extent by their variation in dielectric losses. Finally, the contribution of conducting components such as ions leads to a $1/f$ dependence of the imaginary part of the permittivity. In particular, for biological liquids, which are water based, both the organic and inorganic constituents lead to specific modifications of the frequency dependence of the real and imaginary part of the complex permittivity at microwave frequencies.

Below we discuss the data on selected solutes in water that were measured by our resonator technique. Organic polar and unpolar molecules with slow relaxation time or electrolytes dissolved in water cause a reorientation of intermolecular bonds and result in a change in the frequency dependence of real and imaginary part of permittivity. Therefore we expect that our technique allows observing changes in frequency and inverse quality factor depending on the dissolved species and on concentration with a good accuracy for small droplets.

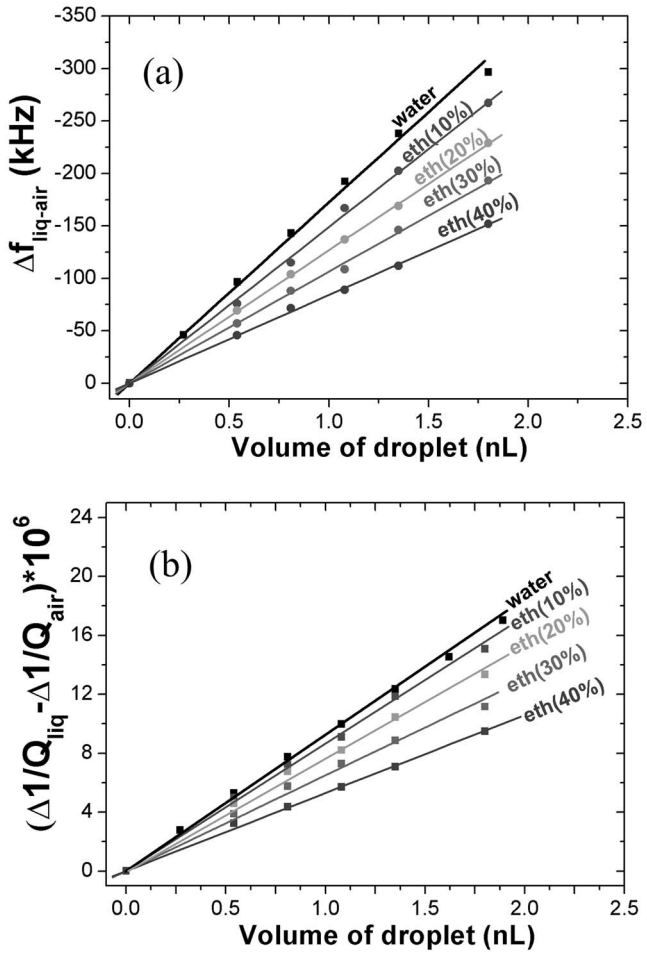

FIG. 5. Measured droplet induced changes in (a) resonant frequency $\Delta f_{\text{liq-air}}$ and (b) inverse quality factor $1/Q_{\text{liq}}-1/Q_{\text{air}}$ as functions of volume of dilute aqueous solutions of ethanol ($T=18$ °C).

A. Examples of nonelectrolyte solutions

In Fig. 5 we compare the dependencies of the droplet induced changes in the resonance properties for diluted aqueous solutions of ethanol of different concentrations C_v. Bidistilled and de-ionized water was used as a reference liquid because it is the most investigated dielectric of all.[19] The results indicate that the resonator allows us to distinguish different concentrations of ethanol in such small volumes. The obtained dependencies tend to be linear on droplet volume for this range, which is advantageous for the calibration of our system.

Now we compare the measured changes in resonant frequency and inverse quality factor with the real and imaginary parts of the complex dielectric permittivity $\varepsilon^*(\omega)$ of diluted aqueous solutions of ethanol, which can be well described by a Debye-type relaxation spectral function reflecting one discrete relaxation time for a binary mixture,[20]

$$\varepsilon_m^*(\omega)=\varepsilon_\infty^m(T)+\frac{\varepsilon_0^m(T)-\varepsilon_\infty^m}{1+i\omega\tau_m(T)}, \quad (1)$$

where ε_∞^m and ε_0^m are the optical and the static dielectric constants of the mixture, respectively, τ_m is the relaxation time of the mixture, and $\omega=2\pi f$ is the angular frequency of the applied field.

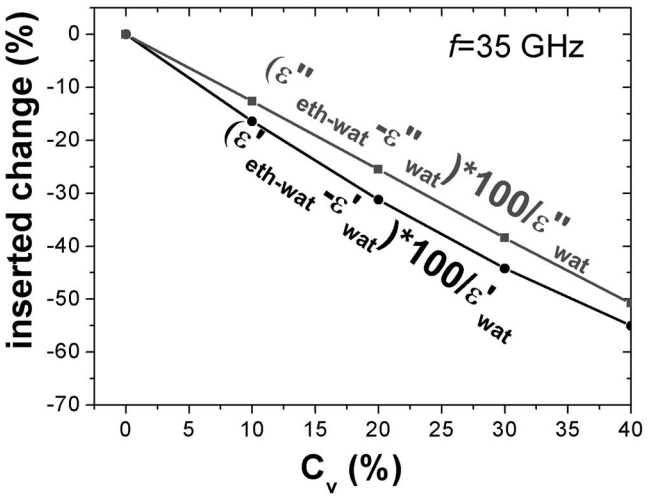

FIG. 6. Calculated dielectric permittivity (real ε' and imaginary ε'' parts) as a function of concentration (C_v) of ethanol in bidistilled water (T=20 °C).

In Fig. 6 we show the data calculated from Eq. (1) for the real and imaginary parts of the complex permittivity as a function of concentration using the parameters of the Debye function displayed for water-ethanol mixtures in tabular format.[20–22] The corresponding values for 35 GHz are represented in the form of relative change (in %) in dielectric permittivity with respect to the permittivity of bidistilled water. The negative sign of the percentage means that adding ethanol to water decreases both real and imaginary parts of $\varepsilon^*(\omega)$.

Since the disturbance of the resonant field induced by the droplet is sufficiently small, a perturbation technique[23] can be applied for system calibration. The effects of ε' and ε'' on the resonance are essentially separated, and each quantity can be determined independently from the measured frequency shift and change in the inverse quality factor of the resonator, respectively.

B. Example of electrolyte solutions

The same technique was applied to investigate a sodium chloride-water solution with 70 parts per thousand (ppt) salinity. The measured linear volume dependencies shown in Fig. 7 allow us to distinguish the solution with this salinity from the reference liquid (water).

The results on the dielectric properties of aqueous electrolytic solutions are of considerable importance because of their relevance for chemical and biological processes, and their influence on the dielectric properties of cells and biological tissue. In many cases, the complex dielectric constant of NaCl-water solution as a function of frequency can be adequately represented by the Debye equation of the following form,[24]

$$\varepsilon_S^*(\omega) = \varepsilon_\infty^w + \frac{\varepsilon_0^S - \varepsilon_\infty^w}{1 - i\omega\tau_S} + i\frac{\sigma}{\varepsilon_0\omega}, \tag{2}$$

where $\varepsilon_0 = 8.854 \times 10^{-12}$ F/m is permittivity of vacuum, ε_∞^w is the high frequency limit of ε_w^* known to be independent on salinity[24] and equal to one of pure (distilled) water, ε_0^S, τ_S, and σ are static dielectric constant, relaxation time, and ionic

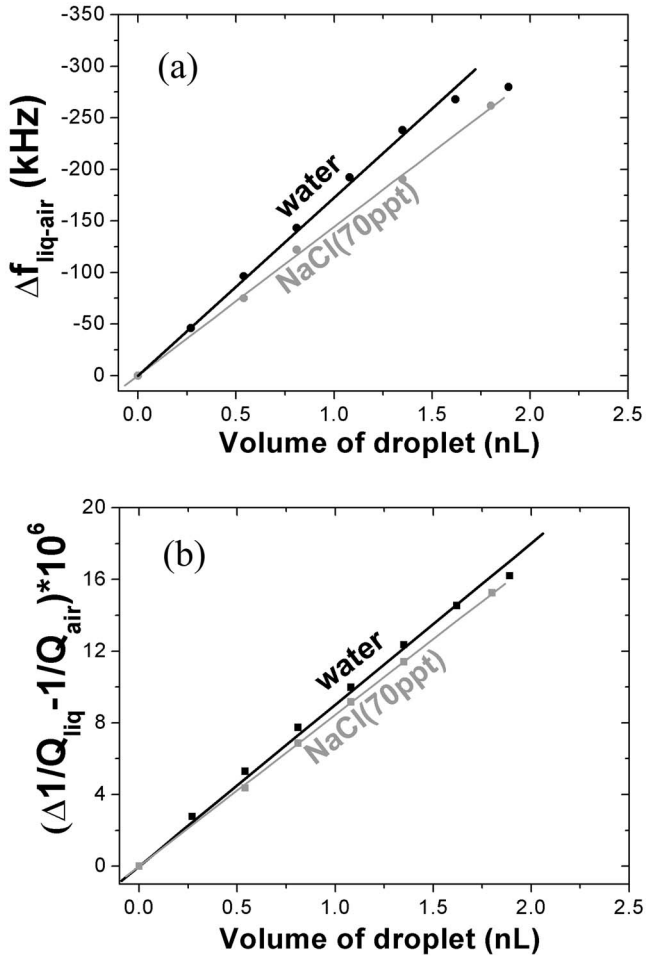

FIG. 7. Measured droplet induced changes in (a) resonant frequency $\Delta f_{\text{liq-air}}$ and (b) inverse quality factor $1/Q_{\text{liq}} - 1/Q_{\text{air}}$ as functions of volume of bidistilled water and aqueous solution of NaCl for a salinity of 70 ppt (T =18 °C).

conductivity of the solution, respectively. These quantities can be expressed in terms of salinity and temperature by the following equations,[24,25]

$$\varepsilon_0^S = \varepsilon_0^w(T)A(T,S); \quad \tau_S = \tau_w(T)B(T,S),$$

$$\sigma = \sigma_{T=25\,^\circ\text{C}}(S)e^{-\varphi(T,S)},$$

where the salinity S is expressed in ppt on a weight basis; $A(T,S)$, $B(T,S)$, and $\varphi(T,S)$ are empirical functions.

In Fig. 8 we present the permittivity data for dilute aqueous solutions of sodium chloride calculated using Eq. (2) for electrolytic solutions. The results demonstrate that the change in ε' corresponding to the frequency shift is more sensitive to increasing salinity than the alteration of ε'' with a corresponding smaller change in the inverse Q-factor. The selected NaCl concentration, which is about seven times higher than in a physiological solution, reveals a small effect on measured parameters. This result gives an advantage for the observation of biological liquids, since the effect of diluted biomolecules may otherwise be masked by the ions.

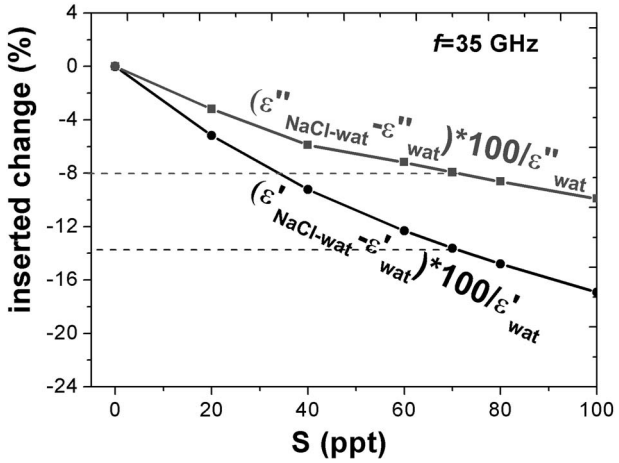

FIG. 8. Calculated dielectric permittivity (real ε' and imaginary ε'' parts) as a function of salinity (S) of NaCl in bidistilled water ($T=18$ °C).

C. Measurements on aqueous solutions of albumin and glucose

The dielectric study of biological complex molecules like proteins and carbohydrates dissolved in water are important since these are essential parts of the living organism and participate in every process within cells. Analysis of these substances has been of ever growing importance because of the simple diagnosis of diseases. Dielectric relaxation spectroscopy of proteins allows studying of the structural properties of proteins in various environmental conditions.

As an example approaching biological liquids, we have started with the investigation of diluted albumin and glucose. In magnitude relation albumin is mostly represented among other proteins and was one of the first proteins to be studied in dielectric spectroscopy experiments.[26] On the other hand, the glucose concentration in blood is of diagnostic relevance in medicine. Glucose serves as a main energy source, used to maintain the structural and functional properties of the cells. Microwave results on various saccharides were reported in Refs. 27 and 28.

Our results depicted in Fig. 9 indicate that for concentrations down to 5% both solutions can be clearly separated from water. Qualitatively, there is a challenging similarity to ethanol and NaCl. Glucose is a complex organic molecule and simply reduces the concentration of "active" water molecules, which absorb electromagnetic energy by the dipole relaxation process. Therefore, both the inverse quality factor and resonant frequency are reduced by the same percentage upon increasing the concentration of the solvent. In contrast, albumin is a charged protein. First, broadband experiments on proteins indicate a $1/f$ part in the imaginary part of the permittivity at low frequencies.[29] According to Fig. 9, the resulting change in the inverse quality factor with increasing concentration of albumin is significantly smaller than for the observed frequency shift.

Hence, due to the linear dependence of the observed frequency shift and change in the inverse quality factor on the volume we may consider the ratio of both quantities as a volume independent measure for the ionic character of the dissolved species in water.

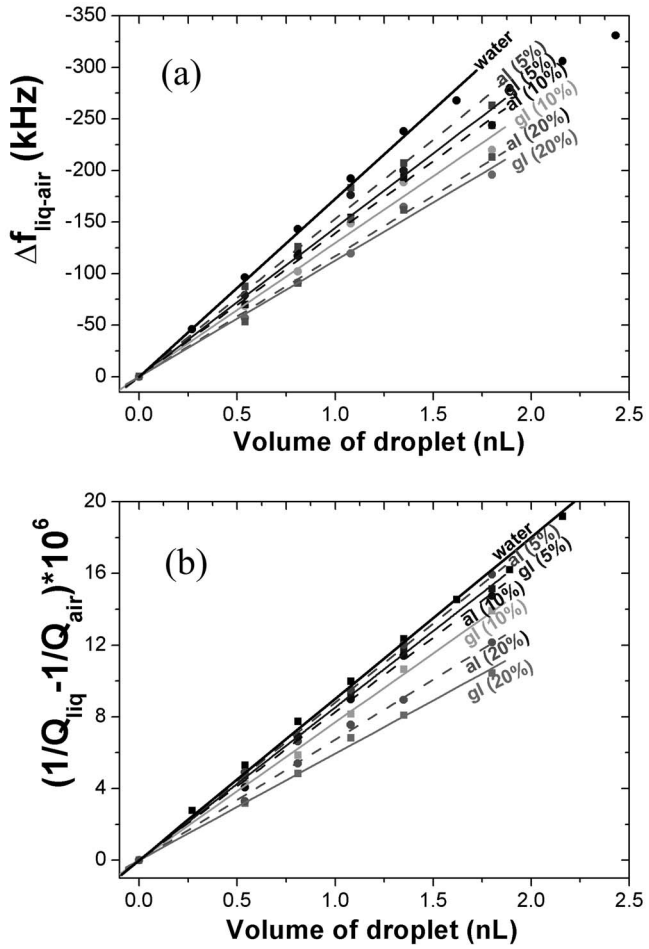

FIG. 9. Measured at $T=18$ °C droplet induced changes in (a) resonant frequency $\Delta f_{\text{liq-air}}$ and (b) inverse quality factor $1/Q_{\text{liq}}-1/Q_{\text{air}}$ as functions of volume of bidistilled water and aqueous solutions of glucose and lactalbumin.

V. CONCLUSIONS

We have developed and optimized an open WGM resonator at millimeter wave frequencies for the characterization of nanoliter droplets of aqueous solutions. Since WGMs in dielectric disks provide the highest Q-factors, they can be used without any shielding as open resonator structures with free access for the sample under investigation, and the evanescent field at the surface can be employed for the sensing of microscopic objects. In order to attain the highest flexibility for controlling and varying the volume of the liquid and for selecting the area on the resonator surface providing the highest sensitivity, we have performed measurements on droplets down to 90 pl volume, which can be applied at arbitrary locations on the resonator surface employing an xy scanning microspotter system. The nearly running waves excited by dielectric image waveguides allow positioning the droplet independently on azimuthal coordinate, which is more convenient for practical applications.

Examples of liquid identification and concentration determination on droplets were presented for ethanol, glucose, albumin, and NaCl dissolved in water. Data on real and imaginary parts of the dielectric permittivity calculated applying Debye relaxation models for binary mixtures of and

literature parameters show the same tendency as our experimental results on frequency shift and change in inverse quality factor. For absolute determination of the permittivity it is important that the volume of the liquid under test is most precisely determined. Combining dielectric resonator sensor with microfluidic systems made from material with low microwave losses will provide a challenging basis for future microfluid-WGM-resonator hybrid systems for biomedical sensing applications.

ACKNOWLEDGMENTS

We would like to acknowledge the help of Dr. Sven Ingebrant, who provided the spotting system, and of Dieter Lomparsky, who was debugging the software for positioning the resonator-pipette-camera system and some other elements of the experimental equipment.

The work was supported in part by an INTAS Fellowship Grant Ref. No. 05-109-4592.

[1]Basics of measuring dielectric properties of materials, Agilent Application Note No. 5989-2589EN, 2005, http://cp.literature.agilent.com/litweb/pdf/5989-2589EN.pdf
[2]M. N. Afsar, N. Suwanvisan, and Y. Wang, Microwave Opt. Technol. Lett. **48**, 275 (2006).
[3]R. Nozaki and T. K. Bose, IEEE Trans. Instrum. Meas. **39**, 945 (1990).
[4]K. Murata, A. Hawana, and R. Nozaki, J. Appl. Phys. **98**, 084107 (2005).
[5]J. C. Booth, J. Mateu, M. Janezic, J. Baker-Jarvis, and J. A. Beall, IEEE MTT-S Int. Microwave Symp. Dig., 4 (2006).
[6]G. R. Facer, D. A. Notterman, and L. L. Sohn, Appl. Phys. Lett. **78**, 996 (2001).
[7]K. B. Yu, S. G. Ogourtsov, V. G. Belenky, A. B. Maslenikov, and A. S. Omar, IEEE Trans. Microwave Theory Tech. **48**, 2159 (2000).
[8]U. Raveendranath, S. Bijukumar, and K. T. Mathew, IEEE Trans. Instrum. Meas. **49**, 1305 (2000).
[9]N. T. Cherpak, A. A. Lavrinovich, and E. N. Shaforost, Int. J. Infrared Millim. Waves **27**, 115 (2006).
[10]J. Krupka, J. Eur. Ceram. Soc. **23**, 2607 (2003).
[11]N. Klein, in *Nanoelectronics and Information Technology*, edited by R. Waser (Wiley, New York, 2003), p. 757.
[12]G. Annino, D. Bertolini, M. Cassetari, M. Fittipaldi, I. Longo, and M. Martinelli, J. Chem. Phys. **112**, 2308 (2000).
[13]R. W. Boyd and J. E. Heebner, Appl. Opt. **40**, 5742 (2001).
[14]S. Arnold, M. Khoshima, I. Teraoka, S. Holler, and F. Vollmer, Opt. Lett. **28**, 272 (2003).
[15]Ch. Y. Chao and L. J. Guo, Appl. Phys. Lett. **83**, 1527 (2003).
[16]Sh. Shindo and I. Itanami, IEEE Trans. Microwave Theory Tech. **26**, 747 (1978).
[17]E. Shaforost, A. Barannik, and N. Klein, Proceedings of the MSMW'07, Kharkov, Ukraine, 2007 (unpublished), Vol. X-24, p. 919.
[18]P. J. Petersan and S. M. Anlage, J. Appl. Phys. **84**, 3392 (1998).
[19]W. J. Ellison, J. Phys. Chem. Ref. Data **36**, 1 (2007).
[20]A. A. Barannik, N. T. Cherpak, Yu. V. Prokopenko, Yu. F. Filipov, E. N. Shaforost, and I. A. Shipilova, Meas. Sci. Technol. **18**, 2231 (2007).
[21]P. Petong, R. Potter, and U. Kaatze, J. Phys. Chem. A **104**, 7420 (2000).
[22]U. Kaatze, Meas. Sci. Technol. **18**, 967 (2007).
[23]J. A. Stratton, *Electromagnetic Theory* (McGraw-Hill, New York, 1941), p. 615.
[24]A. Stogryn, IEEE Trans. Microwave Theory Tech. **19**, 733 (1971).
[25]L. A. Klein and C. T. Swift, IEEE Trans. Antennas Propag. **25**, 104 (1977).
[26]J. L. Oncley, Biophys. Chem. **100**, 151 (2003).
[27]V. V. Meriakri, E. E. Chigrai, D. Kim, I. P. Nikitin, L. I. Pangonis, M. P. Parkhomenko, and J. H. Won, Meas. Sci. Technol. **18**, 977 (2007).
[28]K. Fuchs and U. Kaatze, J. Phys. Chem. B **105**, 2036 (2001).
[29]R. Pethig, Annu. Rev. Phys. Chem. **43**, 177 (1992).